Z. Angew. Math. Phys. (2016) 67:94

0044-2275/16/040001-14
published online July 18, 2016
DOI 10.1007/s00033-016-0687-2

Zeitschrift für angewandte Mathematik und Physik ZAMP

A novel mathematical model for growth of capillaries and nutrient supply with application to prediction of osteophyte onset

Ewa Bednarczyk and Tomasz Lekszycki

Abstract. In this paper, a novel evolution equation for capillaries growth is proposed. An essential ingredient is given by the consideration of nutrient supply, for which a novel constitutive equation is also proposed. The biological and mechanical stimuli are assumed to depend in non-local way on relevant kinematical descriptors. The integro-differential equations governing the system evolution are extremely sensitive to parameter variations. However, it was possible to perform some meaningful numerical simulations in which osteophyte onset has been observed. While the choice of these parameters was judiciously driven by biomechanical "a priori" knowledge, the mathematical problems concerning well-posedness, stability and continuous dependence of solutions seem to be very challenging and will be object of future investigations. This effort seems motivated by the fact that proposed equations are, to our knowledge, the first ones allowing for the prediction of osteophytes onset.

Mathematics Subject Classification. 74-04 · 74L15 · 74S05.

Keywords. Osteoarthritis, Angiogenesis, Mathematical modelling, Mechanical loading.

1. Motivation from biomechanical phenomenology

The osteophytes ingrowth is a part of osteoarthritis (OA) development. This disease involves mechanical and biological factors in the domain close to the surface of cartilage and bone tissue connection. OA is one of the most common diseases that has become social as well as health issue. It predominantly affects the elders but also sportsmen, obese people and those with curvature of the spine. Although the issue is not yet fully understood, mechanical aspects are crucial in the evolution of osteoarthritis. Mechanical overloading leads to chondrocytes apoptosis which increase generation of vascular endothelial growth factors. Consequently, capillaries are going to proliferate and bone cells arrive to invade cartilage. Presence of nutrients from the capillaries and transported and released bone cells creates the environment conductive to osteophytes expansion. It can be seen that presence of capillaries is an inherent part of osteophytes expansion. A healthy working knee joint characterized by a slick surface articular cartilage on the tip of long bone enables regular distribution of the loads and smooth motion.

Previously mentioned cartilage is a flexible connective tissue, avascular and nerveless and thanks to its microstructure reduces friction and absorbs shock during the movement. The articular cartilage is elastic and capable of sustaining shearing forces. On the other side, bone tissue is strong and rigid. The articular cartilage has high tensile strength and is compression resistant (see [1] for a general biological reference and [2,3] for biomechanical models). Long bones are highly vascularized and built with an outer hard layer so-called compact bone and an internal porous spongy tissue with marrow. Main functions of bone are to support a structural framework for the body, protection of internal organs and assisting movement. The aetiology of osteoarthritis is neither uniquely determined nor completely explained. It is not known whether the joint degeneration is a cartilage or a bone disease, but often the osteophytes growth follows inflammation state. It is crucial that osteophytes can develop only with capillaries and nutrients transported by them. Bone cells need nutrients to exist, and the smallest blood vessels–capillaries allow

supply nutrients to the nearest surrounding [4]. The process of development of new blood vessels from the existing vascular network is called angiogenesis or neovascularization. This process is very complex and is involved with physiological and pathological conditions, for example fracture healing or during the development of tumour growth. Angiogenesis does not appear in a state of physiological equilibrium in healthy organisms [5]. Dysfunction of inhibiting and stimulating factors causes the development of new capillaries. Consequently, the neovascularization stimulants are stronger [6]. During osteoarthritis development, an imbalance of factors appears. Mechanically overloaded cartilage chondrocytes start to die and to produce vascular endothelial growth factors (VEGF) which stimulates capillaries to grow [7]. This is happening because of some non-physiology effects. Normally, in healthy cartilage, the amount of VEGF and other angiogenic factors is in an equilibrium state enough to keep balance between bone and cartilage surface. Besides, the absence of capillaries allows for chondrocytes nutrition only via diffusion process. After mechanical overloading resulting from overweight, certain jobs and sports, chondrocytes increase production of VEGF and articular cartilage is unbalanced. As dying cells send signals calling for nutrients, when they are overstressed capillary growth is promoted in their direction, eventually also inside the cartilage. Presence of nutrients from the capillaries and released bone cells creates environment favourable to osteophytes development. The growth of capillaries makes movement difficult and painful. The disease predominantly is associated with ageing but not only. Sex, being overweight, joint injury and its genetic defect as well as stresses in the joints are also very unfavourable and can contribute to the cartilage degeneration [8].

In the literature, a lot of experiments were proposed and reported. Some of them concentrate on mechanical factors and conclude that they are the main reasons of osteoarthritic changes [9–11]. Numerous studies confirmed that the periodic mechanical loading and excessive or non-standard stress [12,13] lead to decrease in shock absorption features and chondrocytes apoptosis [14,15]. Capillaries invasion from bone into the articular cartilage in the late state of disease was also observed [16]. Both mechanical loading and angiogenesis expansion lead to apoptosis of chondrocytes making signals stronger and accelerating joint degeneration [14,17]. In the literature, some theoretical models describing mathematically osteoarthritis in joint were also presented. Some authors concentrate on mechanical aspects of loading and structure of cartilage [18]. However, combination of biomechanical and biochemical models may also be found [19–21], but it was not possible yet to find mathematical models taking into account capillaries ingrowth.

Degenerative joint disease is a very complex case combining biological, chemical and mechanical aspects. Properly formulated mathematical model of cartilage degeneration and osteophytes development including angiogenesis phenomenon can significantly help to comprehend complexity of this process. The presented model reflects the most important aspects of the interaction between mechanical and biological factors crucial for osteoarthritis phenomenon.

2. Mathematical model

2.1. Kinematics

The state of considered system will be characterized by a set of independent fields defined in a reference configuration Ω. The points in Ω represent material particles constituting either bone or cartilage. In the initial configuration which is shown in Fig. 2, the layer C (respectively B) is assumed to be occupied by Cartilage (respectively Bone).

- The first kinematical field introduced is the one describing the evolution of Young modulus. Denoting it by $E(\mathbf{x}, t)$, it has to be remarked that it is assumed it can vary in space and time, so that it is allowed the transformation of the particular particle $\mathbf{x}$ from *cartilage* into *bone*, once the value of $E(\mathbf{x}, t)$ changes correspondingly. Its evolution allows for the distinction of different tissues formed in a given place. So the onset of osteophyte is detected in our model by means of the value attained by E.

- The second considered kinematical field $C(\mathbf{x}, t)$ describes the actual number of bone cells which are present the instant $\mathbf{t}$ at the particular $\mathbf{x}$. Together with Young modulus this field describes the cartilage–bone transition: it is necessary because

  i) its value directly influences the nutrients' supply,
  ii) its value determines nutrients' demand,
  iii) it determines the capacity to built bone.
- Finally, it is introduced the novel field called $B(\mathbf{x}, t)$. It is a scalar field which synthetically describes, roughly speaking, "the volume density" of capillaries present in $\mathbf{x}$ at instant t. The field B is assumed to determine the volume amount of blood which the capillaries can transport through the point $\mathbf{x}$.

  Useless to say considered growth and diffusion phenomena are driven by mechanical deformation (as it is commonly assumed in the literature; see e.g. [22–25]). The only coupling effect which is assumed to be active from biological phenomena to mechanical ones is the biologically driven variation of Young modulus.
- Therefore, the last kinematical field to be introduced will be displacement, denoted by u. It will be considered only the linearized deformation measure ε together with only linear mechanical constitutive equation.

2.2. Dependent fields given by constitutive equation

- Mechanical stress σ is given in terms of deformation measure, ε, as follows

$$\sigma = E\varepsilon, \tag{1}$$

- The biological signal N_s, which was introduced in this work, is proportional to the difference between optimal nutrients consumption and nutrients supply actually transported by capillaries. We postulate the following equation:

$$N_S = \eta_m C(\mathbf{x}, t) - f \int_{\Omega} B(\boldsymbol{\zeta}, t) e^{-\alpha r} d\Omega, \tag{2}$$

  where f is a sensing parameter, which we assume to be constant. Exploration of η_m meaning is included in the discussion of Eq. (6). Finally, the length $1/\alpha$ denotes the exponential decay radius characterizing the region which produces the biological signal.
- The mechanical signal $W_B(\mathbf{x}, t)$ for capillaries growth released by overloaded dying chondrocytes is assumed as the difference between the actual elastic strain energy density $W_s(\mathbf{x}, t)$ and some reference value w_B representing the maximal energy density value acceptable by living cartilage cells,

$$W_B(\mathbf{x}, t) = W_s(\mathbf{x}, t) - w_B. \tag{3}$$

- The signal for Young's modulus changes $W_E(\mathbf{x}, t)$ refers to difference between the actual elastic strain density $W_s(\mathbf{x}, t)$ and the reference value w_E,

$$W_E(\mathbf{x}, t) = W_s(\mathbf{x}, t) - w_E, \tag{4}$$

  where w_E denotes the reference value associated with the equilibrium state of bone remodelling process.

Introduced above parameters w_B and w_E depend on the tissue which is under consideration. The signals $W_B(\mathbf{x}, t)$ and $W_E(\mathbf{x}, t)$ are necessary to formulate evolution equations Eqs. (9) and (11) for capillaries and Young modulus variations, respectively. Because of their definition, it is clear that w_B is greater than w_E.

2.3. Evolution equations

The presented model consists of a system of nonlinear integro-differential equations and a set of different constraints represented by inequalities. The correspondent system of equations and models inequalities interactions between cells, capillaries and nutrients and deformation depends on the tissue mechanical properties.

In the nineteenth century, Verhulst [26] proposed a famous mathematical formula describing the proliferation of cells and inhibition effect of excessive density of cells in culture. This formula was used later in other publications (see eg. Shirsat et al. [27]). Following this idea, it is adopted an equation for the variation of a number of cells $C(\mathbf{x},t)$ in the form,

$$\frac{\partial C(\mathbf{x},t)}{\partial t} = \underbrace{\eta(\mathbf{x},t)C(\mathbf{x},t)}_{(1)} - \underbrace{\tau C^2(\mathbf{x},t)}_{(2)}, \tag{5}$$

where τ denotes a constant parameter, controlling cellular overpopulation.

To specify the role of the field η, it has to be remarked that two effects contribute in the variation of $C(\mathbf{x},t)$. The first one (1), associated with the term $\eta(\mathbf{x},t)C(\mathbf{x},t)$, is responsible for cells proliferation, while negative effect of the interactions between cells is represented by the second one (2). This second effect grows quickly with increasing density of cells. The variable $\eta(\mathbf{x},t)$ denotes the actual consumption of nutrients by a single cell, that is, the mass of nutrients consumed by a cell in unit time and it is defined by the Monod's equation [28],

$$\eta(\mathbf{x},t) = \frac{\eta_m N(\mathbf{x},t)}{K_s + N(\mathbf{x},t)}. \tag{6}$$

Parameter η_m in this equation represents the maximum possible consumption of nutrients by a single cell in the best possible environment and K_s is a positive constant determining the nutrients "scarcity" growth corrective parameter: when $N = K_s$ then the cellular growth rate is exactly half of the optimal one.

In order to include the influence of angiogenesis, the standard formula for the variation $N(\mathbf{x},t)$ is extended in the present formulation and the second term (3) in the following formula representing the supply of nutrients from capillaries is added, as follows

$$\frac{\partial N(\mathbf{x},t)}{\partial t} = -a\eta(\mathbf{x},t)C(\mathbf{x},t) + \underbrace{f\int_{\Omega} B(\boldsymbol{\zeta},t)e^{-\alpha r}d\zeta_1 d\zeta_2 d\zeta_3}_{(3)}. \tag{7}$$

The first, negative part, in Eq. (7) represents the actual consumption of nutrients by the cells at the specific location. The second term (3) with the integral over the tissue domain Ω corresponds to nutrients supply transported by the capillaries in the neighbourhood to the considered location. It has to be recalled that $B(\boldsymbol{\zeta},t)$ denotes the density of capillaries defined by analogy to porosity, tentatively as the ratio of capillaries volume to the total volume of tissue incorporating them. The exponential term approximates decreasing density of nutrients at the distance r from the source.

$$r = \sqrt{(x_1-\zeta_1)^2 + (x_2-\zeta_2)^2 + (x_3-\zeta_3)^2}. \tag{8}$$

The integral enables summation at the certain position $\mathbf{x}$ of the nutrients delivered by surrounding capillaries located at $\boldsymbol{\zeta}$. Coefficients a and f denote weight parameters.

Consequently to the defined assumptions, a novel formula for the rate of the density of capillaries is proposed in the following form,

$$\frac{\partial B(\mathbf{x},t)}{\partial t} = \underbrace{b\overbrace{\int_\Omega B(\boldsymbol{\zeta},t)e^{-\gamma r}d\zeta_1 d\zeta_2 d\zeta_3}^{(*)}\int_\Omega N_S(\boldsymbol{\zeta},t)e^{-\beta r}d\zeta_1 d\zeta_2 d\zeta_3}_{(4)}$$
$$+\underbrace{d\overbrace{\int_\Omega B(\boldsymbol{\zeta},t)e^{-\vartheta r}d\zeta_1 d\zeta_2 d\zeta_3}^{(*)}\int_\Omega W_B(\boldsymbol{\zeta},t)e^{-\xi r}d\zeta_1 d\zeta_2 d\zeta_3}_{(5)}. \tag{9}$$

Last equation is novel. It consists of two different parts representing both playing a relevant role being related to different effects. The coefficients in negative exponents appearing in the previous Eq. (9) characterize the exponential decay range of all considered non-local effects.

The first term (4) depending on N_S defines the development of capillaries caused by the biological signal N_S from the surrounding cells which need nutrients to survive. This signals diminishes with distance from source.

The second one (5) represents the contribution to the development of capillaries caused by the overloaded dying chondrocytes in the cartilage. Remembering about different bone and cartilage stiffness, the evolution of Young's modulus, and consequently density of elastic strain energy, plays a major role. Mechanical signal $W_B(\boldsymbol{\zeta},t)$ is more effective in the nearest area of applied force, and its range of influence decreases with distance from it. Nevertheless, with the grow of the osteophyte domain with bone Young's modulus, the mechanical effect is amplifying. Greater stiffness of a bone tissue and consequently bigger density of elastic strain energy is the final cause of this phenomenon. In both terms, it appears the additional quotient 'scaling' quantity $(*)$ which is given by an integral over the domain of tissue whose integrand depend on B. The so-defined operator reflects the fact that the capillaries' development is only possible in a very close neighbourhood of already existing capillaries network and this effect is non-local in nature. Contribution of mechanical and biological effects is controlled by the parameter d plus those appearing in the definition of the quantity b. Parameter b depends on Young's modulus change. Following the Monod's equation Eq. (6), the relation between parameter b and Young modulus is proposed in the following form

$$b = b_E\left(\frac{E_{max}}{E_{min}+E}\right). \tag{10}$$

In this formula, E_{min} and E_{max} denote minimal and maximal attainable values of Young modulus, respectively, and E represents the actual value of Young modulus.

In the presented equations, signals decrease exponentially with the distance. Parameters $\alpha,\beta,\gamma,\xi,\vartheta$ assign the range of selected signals [22]. The parameters are different from each other and depend on considered effect. It is expected that via the development of presented theory a deeper understanding of the role of these parameters will be gained, so that their experimental determination will become possible. However, the complexity of considered phenomena requires such a modelling complexity. Clearly, approximating with a continuum model systems of such complexity and displaying elaborated internal hierarchies is only possible if a suitably rich model is employed, as it is proved by the great amount of literature on homogenization of microstructures often leading to generalized continuum models (see e.g. [29–35]). Moreover, an even richer model has to be taken into account if one wants to model the presence of synthetic prostheses, in particular for describing the interaction between bone, cartilage and artificial graft (possibly) made of suitable metamaterials (which are indeed increasingly in biomedical applications [36–40]). In this direction, it is clear that a more realistic description can be attained by

means of a microstructure describing the matrix hosting the growth of the capillaries having a suitably rich geometry (useful examples are [41–45]).

The following equation Eq. (11) defines the postulated dependence of Young's modulus evolution on cells density and elastic strain energy density,

$$\frac{\partial E(\mathbf{x},t)}{\partial t} = C(\mathbf{x},t)W_E(\mathbf{x},t). \tag{11}$$

This equation can be interpreted as follows. The living tissue increases (or decreases) its Young's modulus depending on the level of the deformation energy in a neighbourhood of considered material point: if deformation energy is greater than a threshold then the biological response reinforces the tissue, while if the deformation energy is below of the same threshold then the tissue was weakened. Some constraints for E should be introduced namely,

$$E \geq E_{min}, \tag{12}$$

$$E \leq E_{max}. \tag{13}$$

In conclusion, it should be mentioned that the "influence" weighting functions appearing in all introduced integral operators and in particular in Eq. (7) are similar to Green function for diffusion effect adapted to capillaries expansion and signals propagation. Various models have also been proposed including the effects of damage on bone growth [46], a direction that can be very interesting to pursue especially including more refined damage model developed in the meanwhile (see e.g. [47–54]).

3. Predictive numerical simulations

Figure 1 shows the flow chart of the numerical code which is based on a procedure consisting of the following steps:

1. Determination of the initial fields;
2. Mechanical analysis, calculation of actual kinematical descriptors and dependent fields;
3. Calculation of relevant signals;
4. Using the evolution equations with the constraints and the actual values of kinematical descriptors, dependent fields and signals calculation of variations of $B(\mathbf{x},t)$, $C(\mathbf{x},t)$, $N(\mathbf{x},t)$, $E(\mathbf{x},t)$ in the actual time step;

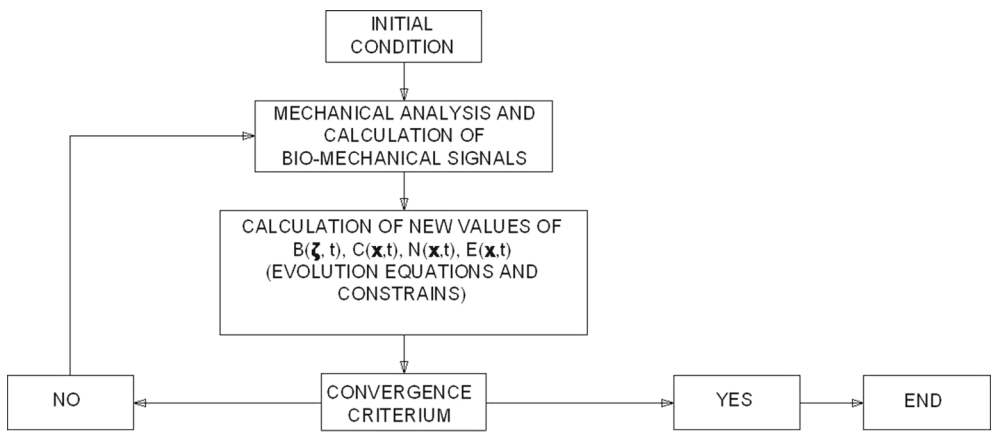

FIG. 1. A scheme of iterative numerical procedure used in an analysis of osteophytes development and considered capillaries expansion

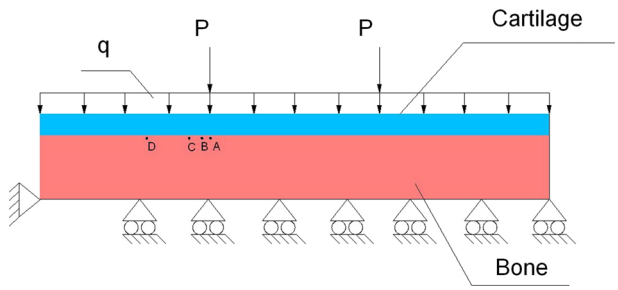

FIG. 2. Schematic geometry considered in numerical examinations

TABLE 1. *Dimensionless value of parameters*

Symbol	α	β	γ	ϑ	ξ	τ	η_m	K_s	a	f	d	w_B	w_E	$E_{\min}$	$E_{\max}$	b_E
Value	17	35	67	17	225	1.5	1.5	2	0.01	1	10^4	5	0.5	0.2	80	5×10^{-4}

5. Calculation of the updated values of $B(\mathbf{x}, t)$, $C(\mathbf{x}, t)$, $N(\mathbf{x}, t)$, $E(\mathbf{x}, t)$;
6. Convergence test and possibly jump to the step (2) if necessary.

A two-dimensional numerical example has been calculated to examine the proposed model and to illustrate some of the effects included in the formulation. Of course less academical, three-dimensional problems need to be studied, possibly exploiting suitable forms of finite element methods able to support the complex constitutive relations needed by the proposed model. Some examples among the huge relevant literature are [55–66]. To follow the changes in capillaries distribution, bone tissue formation and cartilage deterioration triggered by non-uniform mechanical load caused by imperfections of joint external shape, the simple model of an interface between a bone tissue and a cartilage in a joint has been analysed. Let us introduce a rectangle composed of two parts, see Fig. 2. The thick layer represents a domain occupied by a bone tissue. The thinner one represents a cartilage. Due to some imperfections in a joint in addition to the uniform pressure q, this cartilage is loaded by two horizontally oriented forces P applied over two small sub-domains of the external surface. Bone and cartilage tissues are perfectly connected to each other and the domain occupied by a bone tissue as displayed in Fig. 2. The verification if the proposed theoretical model is able to reflect the fundamental effects following clinical observations was the main aim of the presented numerical study. In addition, an examination of influence of selected parameters on osteoarthritic changes was carried out and the basic relations between introduced factors and kinematical descriptors were tested and verified. However, in the future many of the parameters in the model should be estimated experimentally. The values of assumed for the calculations parameters are given in Table 1.

The formulas introduced in the previous section were implemented in the software COMSOL [67] in order to examine the process present at the interface between the bone and the cartilage after application of the non-uniform mechanical load acting on the external surface of the cartilage. Several crucial effects and associated parameters affect the changes in the tissues. The non-uniform mechanical loading applied to the external surface of the cartilage causes concentrations of strain, stress and associated density of strain energy. Excessive loading leads of some of the chondrocytes in the cartilage to death. This phenomenon activates a complex chain of signalling which among the others promotes ingrowth of capillaries into the cartilage domain. Among numerous factors that control this effect some appear to play a crucial role: (a) the extent of the sub-domain surrounding dying cells where the signals are strong enough to activate biochemical reaction of the tissue and capillaries development; (b) the domain of the surroundings capillaries where the system of capillaries can grow from; (c) the level of mechanical load (represented by density of strain energy) which can be accepted by living chondrocytes; (d) the reference value of stimulus regulating bone tissue remodelling. Since the present paper represents the

theoretical study, numerical tests have been performed to get an idea how each of this parameters affect the process. In addition to the already mentioned effects, there are some other which regulate activity and quantity of bone cells involved in osteophytes development. Among them, the parameters defining the consumption of nutrients by cells and factors regulating the distribution of nutrients in the tissue play the most important role. Changes in bone–cartilage composite stiffness following the osteophytes development affect the distribution of strain energy. The stiffnesses of osteophytes and cartilage differ very much from each other. It results in energy concentration in the region surrounding osteophytes. This effect promotes further development of osteophytes. According to the proposed model, this variable in time and space distribution of strain energy has contribution in both biological and mechanical signals in regulation of angiogenesis and osteophytes growth.

In the numerical calculations, dimensionless values were considered and only mutual relations between densities of cells, capillaries and mechanical loading have been examined. In the presented figures, the changes associated with ingrowth of bone tissue into cartilage domain close to the concentrated mechanical loading are displayed. The left-hand side area of the geometry abundant in bone cells represents a healthy bone tissue. The right-hand side poorly populated by bone cells and capillaries represents a cartilage tissue (Fig. 3).

Many numerical calculations were necessary to perform parameter study and to adjust values of parameters. Consequently, some distribution of cells and capillaries at the initial state in the bone and cartilage domains was assumed. It was presumed that the concentration of cells in bone domain is much greater than the cells concentration in the cartilage area $C_B(0) \gg C_C(0)$. Similar assumption was done for concentration of capillaries $B_B(0) \gg B_C(0)$.

In the cartilage domain, tissue degeneration can be observed. Some osteophytes are growing after capillaries expansion. This effect is caused by the angiogenic signals sent from mechanically loaded chondrocytes. Thereafter, growth of bone tissue accompanied by development of capillaries and evolving nutrients concentration takes place.

In addition, an analysis of involvement of selected parameters in angiogenesis and osteophytes development in the aftermath was performed. The examination of time evolution of cell concentration for selected combinations of values of parameters β and ξ in four test points located in the cartilage domain was performed (see Fig. 4). All of this four points are located in the cartilage close to the interface with bone. First point (A) is placed at the action line of concentrated force. The most distant from the symmetry axis point (D) is located sufficiently far from the border of the sample to avoid effect of boundary condition (see Fig. 2).

Figure 4a reflects the variation of density of cells C for $\xi = 225, \beta = 35$. Next three figures represent the situations for $\xi = 247.5, \beta = 35$ (4b), $\xi = 225, \beta = 38.5$ (4c), $\xi = 247.5, \beta = 38.5$ (4d). It follows from the analysis of this results that the farther from concentrated force the value of C is smaller. It can be observed that with growing distance of the test points from the force action line the effects of mechanical and biological signals wane. It follows from the numerical analysis that the effect of ξ is greater compared to the effect of β.

4. Conclusions and future developments

In this paper, a set of coupled integro-differential equations and inequalities is proposed to describe the process of the osteophytes ingrowth for instance during the degenerative joint disease driven by mechanical loading. Particular focus is placed on the role played in this phenomenon by capillaries' growth. Presented novel equations complement already generally accepted mathematical model for describing angiogenesis expansion and osteophytes development. Using formulated model in numerical simulations allowed for the determination of some basic information about relations and connections between selected factors in the process of osteoarthritic degeneration. The results are associated with clinical observations which

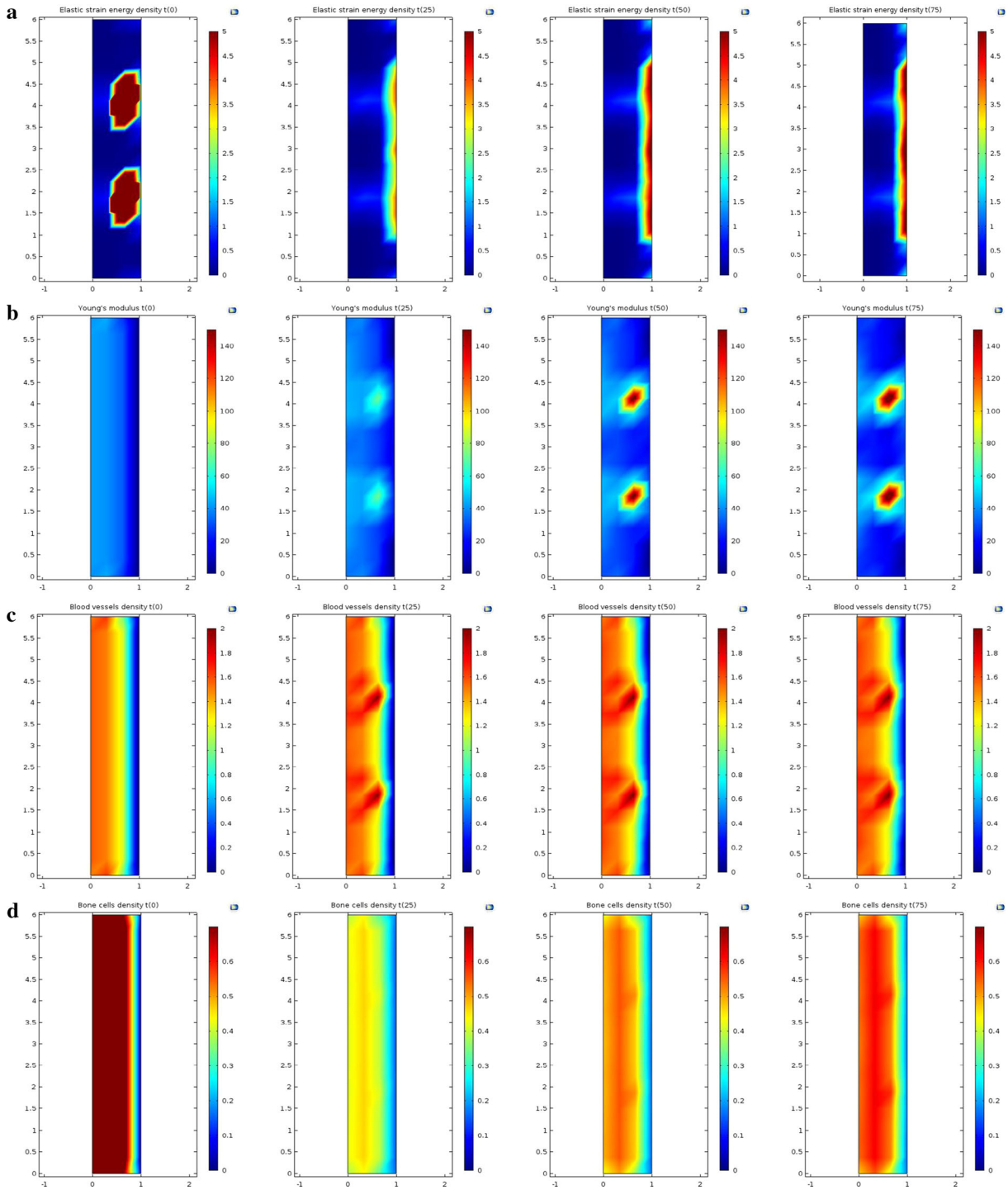

FIG. 3. Comparison of the changes in **a** elastic strain energy density, **b** Young's modulus, **c** capillaries density and **d** bone cells density distribution in time

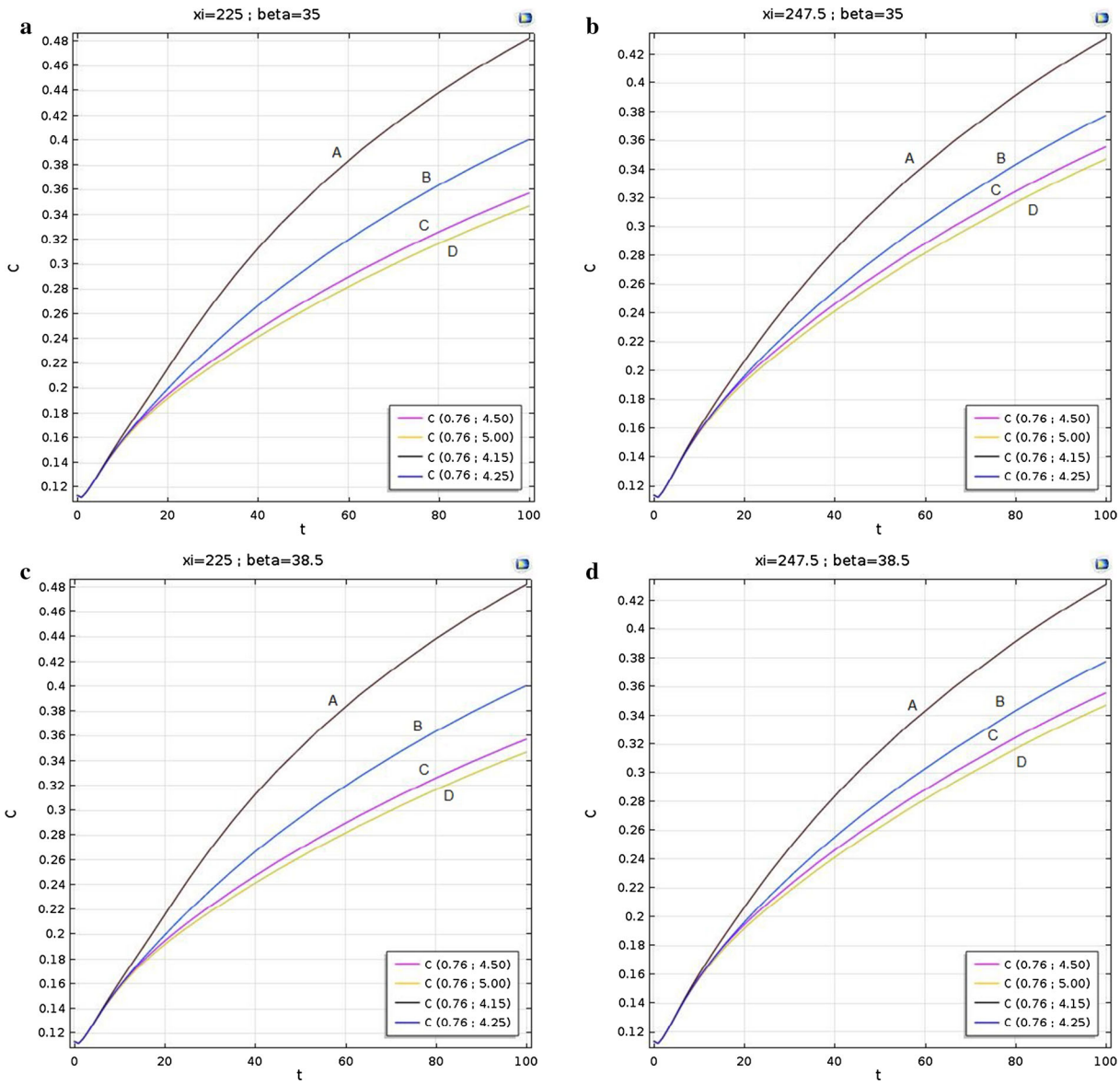

FIG. 4. Evolution in time and change of bone cells density with distance from concentrated force

confirm neovascularization inseparability from osteogenesis. Additionally, both mechanical and biological effects counted in the formulation influence the OA process. Complicated nature of equations and a large number of parameters causes sensitivity of results on small variation of the parameters and numerical instability.

The mathematical model presented here shows some features which render the solution of related problems rather difficult. The reader should not be surprised by this circumstance, as the complexity of described physical phenomena (using the etymological Greek meaning of physics we consider biological phenomena as part of physics) cannot be modelled by means of simple models. The contrary should be considered a weakness of modelling procedure.

The set of novel integro-differential equation put forward here cannot be easily framed into the scope of already available theorems of existence and uniqueness. Even more difficult seems to us the possibility to prove continuum dependence on initial and boundary data or on constitutive parameters. It was possible, by using the robust numerical codes supplied by COMSOL, however, to find the described predictions which support the validity of the proposed model. On the other hand, it was possible to detect the signs characteristic of bifurcation of the solutions (and therefore the corresponding buckling phenomena). Indeed, varying some parameters it was possible for instance to allow for or vice versa to stop the growth of osteophytes.

The stability relative to the system of equations made the development of the code very laborious as well as its application to applicable cases.

The relative problems were overcome by patient calibration of the numerical tool but require for sure the development and application of suitable mathematical tools and results specifically intended to treat complex stability issues (see e.g. [68–74]).

The main features of the model are: (i) its strong (maybe formidable) nonlinearity and (ii) its unremovable non-local structure. These features reflect the physics whose description is attempted and open in our opinion fields of novel mathematical research.

Seen the interesting results presented here, it seems of interest to continue the modelling activity by describing in a more accurate way the related deformation phenomena, by including: (i) geometrical and material nonlinearities [75], (ii) non-isotropic constitutive equations, (iii) varying loads situations in quasi-static or dynamical regimes, (iv) possible presence of prestress, (v) second and higher gradient or microstructured continuum models [76]. In particular, we are aware of the extreme simplification involved in the assumption assuming that the introduced continuum is a standard first gradient one and that the stress–strain relationship is linear: indeed, it is well known that such simplification does not allow for the description of important phenomena involving living tissues. However, the aim of the present paper was to prove that complex non-local biological phenomena involved in tissue growth can be successfully described.

Even richer are the possible developments concerning the modelling of biological phenomena. It is possible to guess that it will be relatively simple to include in the model: (i) a more general directional description of capillaries growth, (ii) a more detailed description of nutrient supply diffusion and (iii) a more complex non-local description of evolution of mechanical properties (see e.g. peridynamic models discussed in [77–79]).

References

1. Howell, D.S.: Biology of Cartilage Cells. Cambridge University Press, Cambridge (1979)
2. Federico, S., Grillo, A.: Elasticity and permeability of porous fibre-reinforced materials under large deformations. Mech. Mater. **44**, 58–71 (2012)
3. Tomic, A., Grillo, A., Federico, S.: Poroelastic materials reinforced by statistically oriented fibres - numerical implementation and application to articular cartilage. IMA J. Appl. Math. **79**, 1027–1059 (2014)
4. Cowin, S.B., Doty, S.C.: Tissue Mechanics. Springer, New York (2007)
5. Maragoudakis, M.E., Gullino, P., Lelkes, P.I. (eds.): Angiogenesis in health and disease. Springer, Berlin (1992)
6. Dvorak, H.F.: Tumors: wounds that do not heal. N. Engl. J. Med. **315**(26), 1650–1659 (1986)
7. Pufe, T., Lemke, A., Kurz, B., Petersen, W., Tillmann, B., Grodzinsky, A.J., Mentlein, R.: Mechanical overload induces VEGF in cartilage discs via hypoxia-inducible factor. Am. J. Pathol. **164**(1), 185–192 (2004)
8. Sharma, L., Berenbaum, F.: Osteoarthritis A Companion to Rheumatology. Elsevier, New York (2007)
9. Hayami, T., Pickarski, M., Zhuo, Y., Wesolowski, G.A., Rodan, G.A., Duong, L.T.: Characterization of articular cartilage and subchondral bone changes in the rat anterior cruciate ligament transection and meniscectomized models of osteoarthritis. Bone **38**, 234–243 (2006)
10. Felson, D.T.: Osteoarthritis as disease of mechanics. Osteoarthr. Cartil. **21**, 10–15 (2013)
11. Wang, T.M., Wu, K.W., Chen, C.R., Hong, S.W., Lu, T.W., Kuo, K.N., Huang, S.C.: Loading rates during walking in adolescents with type ii osteonecrosis secondary to pelvic osteotomy. J. Orthop. Res. (2016). doi:10.1002/jor.23239

12. Findlay, D.M., Atkins, G.J.: Osteoblast-chondrocyte interactions in osteoarthritis. Curr. Osteop. Rep. **12**, 127–134 (2014)
13. Gilbertson, M.M.: Development of periarticular osteophytes in experimentally induced osteoarthritis in the dog. Ann. Rheum. Dis. **34**, 12–25 (1975)
14. D'Lima, D.D., Hashimoto, S., Chen, P.C., Colwell, C.W., Lotz, M.K.: Human chondrocyte apoptosis in response to mechanical injury. Osteoarthr. Cartil. **9**, 712–719 (2001)
15. Kuhn, K., D'Lima, D.D., Hashimoto, S., Lotz, M.: Cell death in cartilage. Osteoarthr. Cartil. **12**, 1–16 (2004)
16. Pfander D., Körtje D., Zimmermann R., Weseloh G., Kirsch T., Gesslein, M., Cramer, T., Swoboda, B.: Vascular endothelial growth factor in articular cartilage of healthy and osteoarthritic human knee joints. Ann. Rheum. Dis. **60**(11), 1070–1073 (2001)
17. Loening, A.M., James, I.E., Levenston, M.E., Badger, A.M., Frank, E.H., Kurz, B., Nuttall, H.H., Hung, M.E., Blake, S.M., Grodzinsky, A.J., Lark, M.W.: Injurious mechanical compression of bovine articular cartilage induces chondrocyte apoptosis. Arch. Biochem. Biophys. **381**, 205–212 (2000)
18. Wu, J.Z., Herzog, W., Epstein, M.: Joint contact mechanics in the early stages of osteoarthritis. Med. Eng. Phys. **22**, 1–12 (2000)
19. Smith, D.W., Gardiner, B.S., Davidson, J.B., Grodzinsky, A.J.: Computational model for the analysis of cartilage and cartilage tissue constructs. J. Tissue Eng. Regen. Med. **10**(4), 334–47 (2014)
20. Manzano, S., Gaffney, E.A., Doblaré, M., Doweidar, M.H.: Cartilage dysfunction in ALS patients as side effect of motion loss: 3d mechano-electrochemical computational model. BioMed. Res. Int. **2014**, 179070-1–179070-13 (2014). doi:10.1155/2014/179070
21. Manzano, S., Doblaré, M., Doweidar, M.H.: Parameter-dependent behavior of articular cartilage: 3d mechano-electrochemical computational model. Comput. Methods Progr. Biomed. **122**(3), 491–502 (2015)
22. Lekszycki, F., dell'Isola, T.: A mixture model with evolving mass densities for describing synthesis and resorption phenomena in bones reconstructed with bio-resorbable materials. ZAMM **92**(6), 426–444 (2012)
23. Giorgio, I., Andreaus, U., Scerrato, D., dell'Isola, F.: A visco-poroelastic model of functional adaptation in bones reconstructed with bio-resorbable materials. Biomech Model. Mechanobiol. (2016). doi:10.1007/s10237-016-0765-6
24. Giorgio, I., Andreaus, U., Scerrato, D., Braidotti, P.: Modeling of a non-local stimulus for bone remodeling process under cyclic load: Application to a dental implant using a bioresorbable porous material. Math. Mech. Solids (2016). doi:10.1177/1081286516644867
25. Andreaus, U., Giorgio, I., Madeo, A.: Modeling of the interaction between bone tissue and resorbable biomaterial as linear elastic materials with voids. Z. Angew. Math. Phys. **66**(1), 209–237 (2015)
26. Verhulst, P.F.: Deuxième mémoire sur la loi d'accroissement de la population. Mémoires de l'Académie Royale Des Sciences, Des Lettres Et Des Beaux-Arts de Belgique **20**, 1–32 (1847)
27. Shirsat, N., Mohd, A., Whelan, J., English, N.J., Glennon, B., Al-Rubeai, M.: Revisiting Verhulst and Monod models: analysis of batch and fed-batch cultures. Cytotechnology **67**, 515–530 (2014)
28. Monod, J.: The growth of bacterial cultures. Ann. Rev. Microbiol. **3**, 371–394 (1949)
29. Carcaterra, A., dell'Isola, F., Esposito, R., Pulvirenti, M.: Macroscopic description of microscopically strongly inhomogenous systems: A mathematical basis for the synthesis of higher gradients metamaterials. Arc. Ration. Mech. Anal. **218**(3), 1239–1262 (2015)
30. Alibert, J.-J., Seppecher, P., dell'Isola, F.: Truss modular beams with deformation energy depending on higher displacement gradients. Math. Mech. Solids **8**(1), 51–73 (2003)
31. Alibert, J.-J., Della Corte, A.: Second-gradient continua as homogenized limit of pantographic microstructured plates: a rigorous proof. Z. Angew. Math. Phys. **66**(5), 2855–2870 (2015)
32. Cecchi, A., Rizzi, N.L.: Heterogeneous elastic solids: a mixed homogenization-rigidification technique. Int. J. Solids Struct. **38**(1), 29–36 (2001)
33. dell'Isola, F., Giorgio, I., Pawlikowski, M., Rizzi, N.L.: Large deformations of planar extensible beams and pantographic lattices: Heuristic homogenisation, experimental and numerical examples of equilibrium. Proc. R. Soc. London A **472**, 20150790 (2016)
34. AminPour, H., Rizzi, N.: A one-dimensional continuum with microstructure for single-wall carbon nanotubes bifurcation analysis. Math. Mech. Solids **21**(2), 168–181 (2016)
35. Aminpour, H., Rizzi, N.: On the modelling of carbon nano tubes as generalized continua. Adv. Struct. Mater. **42**, 15–35 (2016)
36. Del Vescovo, D., Giorgio, I.: Dynamic problems for metamaterials: review of existing models and ideas for further research. Int. J. Eng. Sci. **80**, 153–172 (2014)
37. dell'Isola, F., Steigmann, D., Della Corte, A.: Synthesis of fibrous complex structures: Designing microstructure to deliver targeted macroscale response. Appl. Mech. Rev. **67**(6), 060804 (2015)
38. Altenbach H., Eremeyev, V.A.: Mechanics of viscoelastic plates made of FGMs. In: Murín, J., Kompiš, V., Kutiš, V. (eds.) Computational Modelling and Advanced Simulations. Computational Methods in Applied Sciences, vol. 24, pp. 33–48. Springer, Netherlands (2011). doi:10.1007/978-94-007-0317-9_2

39. Altenbach, H., Eremeyev, V.A.: Strain rate tensors and constitutive equations of inelastic micropolar materials. Int. J. Plast. **63**, 3–17 (2014)
40. Placidi, L., Giorgio, I., Della Corte, A., Scerrato, D.: Euromech 563 Cisterna di Latina 17–21 March 2014 Generalized continua and their applications to the design of composites and metamaterials: a review of presentations and discussions. Math. Mech. Solids (2015). doi:10.1177/1081286515576948
41. Turco, E., dell'Isola, F., Cazzani, A., Rizzi, N.L.: Hencky-type discrete model for pantographic structures: numerical comparison with second gradient continuum models. Z. angew. Math. Phys. (2016). doi:10.1007/s00033-016-0681-8
42. Scerrato, D., Giorgio, I., Rizzi, N.L.: Three-dimensional instabilities of pantographic sheets with parabolic lattices: numerical investigations. Z. Angew. Math. Phys. **67**(3), 1–19 (2016). doi:10.1007/s00033-016-0650-2
43. Scerrato, D., Zhurba Eremeeva, I.A., Lekszycki, T., Rizzi, N.L.: On the effect of shear stiffness on the plane deformation of linear second gradient pantographic sheets. ZAMM Z. Angew. Math. Mech. (2016). doi:10.1002/zamm.201600066
44. Gabriele, S., Rizzi, N., Varano, V.: A 1D nonlinear TWB model accounting for in plane cross-section deformation. Int. J. Solids Struct. (2015). doi:10.1016/j.ijsolstr.2016.04.017
45. Aminpour, H., Rizzi, N.: On the continuum modelling of carbon nano tubes. In: Kruis, J., Tsompanakis, Y., Topping, B.H.V. (eds.) Proceedings of the fifteenth international conference on civil, structural and environmental engineering computing, Paper 240. Civil-Comp Press, Stirlingshire, UK (2015). doi:10.4203/ccp.108.240
46. Prendergast, P.J., Taylor, D.: Prediction of bone adaptation using damage accumulation. J. Biomech. **27**(8), 1067–1076 (1994)
47. D'Annibale, F., Luongo, A.: A damage constitutive model for sliding friction coupled to wear. Contin. Mech. Thermodyn. **25**(2-4), 503–522 (2013)
48. Contrafatto, L., Cuomo, M.: A framework of elastic–plastic damaging model for concrete under multiaxial stress states. Int. J. Plast. **22**(12), 2272–2300 (2006)
49. Placidi, L.: A variational approach for a nonlinear 1-dimensional second gradient continuum damage model. Contin. Mech. Thermodyn. **27**(4), 623–638 (2015)
50. Placidi, L.: A variational approach for a nonlinear one-dimensional damage-elasto-plastic second-gradient continuum model. Contin. Mech. Thermodyn. **28**, 119–137 (2016)
51. Yang, Y., Ching, W.Y., Misra, A.: Higher-order continuum theory applied to fracture simulation of nanoscale intergranular glassy film. J. Nanomech. Micromech. **1**(2), 60–71 (2011)
52. Yang, Y., Misra, A.: Higher-order stress-strain theory for damage modeling implemented in an element-free Galerkin formulation. Comput. Model. Eng. Sci. (CMES) **64**(1), 1–36 (2010)
53. Contrafatto, L., Cuomo, M., Fazio, F.: An enriched finite element for crack opening and rebar slip in reinforced concrete members. Int. J. Fract. **178**(1-2), 33–50 (2012)
54. Cuomo, M., Nicolosi, A.: A poroplastic model for hygro-chemo-mechanical damage of concrete. In: EURO-C; Computational modelling of concrete structures Conference, EURO-C; Computational modelling of concrete structures, pp. 533–542, (2006)
55. Vilanova, G., Colominas, I., Gomez, H.: Capillary networks in tumor angiogenesis: From discrete endothelial cells to phase-field averaged descriptions via isogeometric analysis. Int. J. Numer. Methods Biomed. Eng. **29**(10), 1015–1037 (2013)
56. Bilotta, A., Formica, G., Turco, E.: Performance of a high-continuity finite element in three-dimensional elasticity. Int. J. Numer. Methods Biomed. Eng. **26**(9), 1155–1175 (2010)
57. Cazzani, A., Malagù, M., Turco, E., Stochino, F.: Constitutive models for strongly curved beams in the frame of isogeometric analysis. Math. Mech. Solids **21**(2), 182–209 (2016)
58. Turco, E.: Tools for the numerical solution of inverse problems in structural mechanics: review and research perspectives. European J. Environ. Civil Eng. (2016). doi:10.1080/19648189.2015.1134673
59. Cazzani, A., Malagù, M., Turco, E.: Isogeometric analysis of plane-curved beams. Math. Mech. Solids **21**(5), 562–577 (2014)
60. Cazzani, A., Stochino, F., Turco, E.: An analytical assessment of finite element and isogeometric analyses of the whole spectrum of Timoshenko beams. ZAMM J. Appl. Math. Mech./Z. Angew. Math. Mech. (2016). doi:10.1002/zamm.201500280
61. Ciancio, D., Carol, I., Cuomo, M.: A method for the calculation of inter-element stresses in 3D. Comput. Methods Appl. Mech. Eng. **254**, 222–237 (2013)
62. Greco, L., Cuomo, M.: An isogeometric implicit G1 mixed finite element for Kirchhoff space rods. Comput. Methods Appl. Mech. Eng. **298**, 325–349 (2016)
63. Greco, L., Cuomo, M.: On the force density method for slack cable nets. Int. J. Solids Struct. **49**(13), 1526–1540 (2012)
64. Greco, L., Cuomo, M.: Consistent tangent operator for an exact kirchhoff rod model. Contin. Mech. Thermodyn. **27**(4–5), 861–877 (2015)
65. Cazzani, A., Garusi, E., Tralli, A., Atluri, S.N.: A four-node hybrid assumed-strain finite element for laminated composite plates. CMC Comput. Mater. Contin. **2**(1), 23–38 (2005)

66. Cazzani, A., Lovadina, C.: On some mixed finite element methods for plane membrane problems. Comput. Mech. **20**(6), 560–572 (1997)
67. COMSOL Multiphysics® v. 5.2. www.comsol.com. COMSOL AB, Stockholm, Sweden
68. Piccardo, G., D'Annibale, F., Zulli, D.: On the contribution of Angelo Luongo to mechanics: in honor of his 60th birthday. Contin. Mech. Thermodyn. **27**(4–5), 507–529 (2015)
69. Luongo, A., Zulli, D., Piccardo, G.: A linear curved-beam model for the analysis of galloping in suspended cables. J. Mech. Mater. Struct. **2**(4), 675–694 (2007)
70. Ruta, G.C., Varano, V., Pignataro, M., Rizzi, N.L.: A beam model for the flexural-torsional buckling of thin-walled members with some applications. Thin-Walled Struct. **46**(7), 816–822 (2008)
71. Rizzi, N.L., Varano, V.: The effects of warping on the postbuckling behaviour of thin-walled structures. Thin-Walled Struct. **49**(9), 1091–1097 (2011)
72. Rizzi Nicola, L., Varano, Valerio, Gabriele, Stefano: Initial postbuckling behavior of thin-walled frames under mode interaction. Thin-Walled Struct. **68**, 124–134 (2013)
73. Gabriele, S., Rizzi, N.L., Varano, V.: A one-dimensional nonlinear thin walled beam model derived from Koiter shell theory. In: Topping, B.H.V., Iványi, P. (eds.) Proceedings of the twelfth international conference on computational structures technology, Paper 156. Civil-Comp Press, Stirlingshire, UK (2014). doi:10.4203/ccp.106.156
74. Rizzi, N.L., Varano, V.: On the postbuckling analysis of thin-walled frames. In: Proceedings of the 13th International Conference on Civil, Structural and Environmental Engineering Computing, p. 14, Chania, Crete, Greece (2011)
75. Oliveto, G., Cuomo, M.: Incremental analysis of plane frames with geometric and material nonlinearities. Eng. Struct. **10**(1), 2–12 (1988)
76. Auffray, N., dell'Isola, F., Eremeyev, V.A., Madeo, A., Rosi, G.: Analytical continuum mechanics a la Hamilton-Piola least action principle for second gradient continua and capillary fluids. Math. Mech. Solids **20**(4), 375–417 (2015)
77. dell'Isola, F., Della Corte, A., Esposito, R., Russo, L.: Some cases of unrecognized transmission of scientific knowledge: From antiquity to Gabrio Piola's peridynamics and generalized continuum theories. In: Generalized Continua as Models for Classical and Advanced Materials, pp. 77–128. Springer (2016)
78. dell'Isola, F., Andreaus, U., Placidi, L.: At the origins and in the vanguard of peridynamics, non-local and higher-gradient continuum mechanics: An underestimated and still topical contribution of Gabrio Piola. Math. Mech. Solids **20**(8), 887–928 (2015)
79. dell'Isola, F., Della Corte, A., Giorgio, I.: Higher-gradient continua: The legacy of Piola, Mindlin, Sedov and Toupin and some future research perspectives. Math. Mech. Solids. (2016). doi:10.1177/1081286515616034

Ewa Bednarczyk and Tomasz Lekszycki
Warsaw University of Technology
Warsaw, Poland
e-mail: e.bednarczyk.wpt@gmail.com

(Received: June 2, 2016; revised: June 29, 2016)